Non-Gaussianity from features in the power spectrum

S. Basu,[1,*] D. J. Brooker,[2,†] N. C. Tsamis,[3,‡] and R. P. Woodard[1,§]

[1]*Department of Physics, University of Florida, Gainesville, Florida 32611, USA*
[2]*U.S. Naval Research Laboratory, Code 7160, 4555 Overlook Avenue, SW, Washington, DC 20375, USA*
[3]*Institute of Theoretical Physics & Computational Physics, Department of Physics, University of Crete, GR-710 03 Heraklion, Greece*

(Received 29 May 2019; published 20 September 2019)

The strongest non-Gaussianity in single-scalar potential models of inflation is associated with features in the power spectrum. We stress the importance of accurately modeling the expected signal in order for the standard estimator to minimize contamination by random noise. We present explicit formulas that improve on the approximation introduced by Adshead, Hu, Dvorkin, and Peiris. We also compare with a simple, analytic model of the first feature, and quantify our results using the correlators of Hung, Fergusson, and Shellard.

DOI: 10.1103/PhysRevD.100.063525

I. INTRODUCTION

The prediction of primordial scalar perturbations [1] in single-scalar inflation described by the Lagrangian,

$$\mathcal{L} = \frac{R\sqrt{-g}}{16\pi G} - \frac{1}{2}\partial_\mu\varphi\partial_\nu\varphi g^{\mu\nu}\sqrt{-g} - V(\varphi)\sqrt{-g}, \quad (1)$$

represents the first (and so far the only to our knowledge) observed quantum gravitational phenomenon [2–4]. It is frustrating that we do not know the scalar potential $V(\varphi)$, or even if single-scalar inflation is correct. It is also frustrating that so little guidance for fundamental theory is provided by observation. The approximately 10^7 pixels of data from the primordial spectrum [5] seem to be well described by just two numbers,

$$\Delta^2_{\mathcal{R}}(k) \simeq A_s\left(\frac{k}{k_*}\right)^{n_s-1}, \qquad A_s = (2.105 \pm 0.030)\times 10^{-9},$$
$$n_s = 0.9665 \pm 0.0038, \quad (2)$$

where the pivot is $k_* = 0.05\ \mathrm{Mpc}^{-1}$.

If relation (2) is correct, then we can reconstruct the inflationary geometry in terms of A_s, n_s, and the still unknown tensor-to-scalar ratio $r_* < 0.07$ [6]. Expressing the first slow roll parameter $\epsilon(n)$ and the Hubble parameter $H(n)$ in terms of the number of e-foldings $\Delta n \equiv n - n_*$ since the pivot mode experienced horizon crossing, the lowest order slow roll approximation gives

$$\epsilon(n) \simeq \frac{r_*}{16}e^{(1-n_s)\Delta n},$$
$$H(n) \simeq H_*\exp\left[-\frac{r_*}{16(1-n_s)}(e^{(1-n_s)\Delta n}-1)\right], \quad (3)$$

where $8\pi G H_*^2 \equiv r_* A_s \pi^2/2$. Using the standard procedure for reconstructing the inflaton and its potential [7–12], we find

$$\sqrt{8\pi G}(\varphi(n)-\varphi_*) \equiv \Delta\psi \simeq -\frac{1}{1-n_s}\sqrt{\frac{r_*}{2}}[e^{\frac{1}{2}(1-n_s)\Delta n}-1], \quad (4)$$

$$(8\pi G)^2 V(\varphi) \simeq \frac{3}{2}\pi^2 r_* A_s \exp\left[\sqrt{\frac{r_*}{8}}\Delta\psi - \left(\frac{1-n_s}{4}\right)\Delta\psi^2\right]. \quad (5)$$

Nature is under no compulsion to comply with human aesthetic prejudices, so the featureless, gently sloping potential (5) may be all there is to primordial inflation. However, it raises severe issues with the fine-tuning of initial conditions needed to make inflation start, and with the tendency for small fluctuations to produce dramatically different conditions in distant portions of the universe [13]. What to make of this has provoked controversy even among some of the pioneers of inflation [14–16].

The power spectrum data [17] actually provide marginal evidence for more structure in the form of "features." These are transient fluctuations away from the best fit—usually a depression of power followed by an excess at smaller angular scales—which are visible in the Planck residuals for $20 \lesssim \ell \lesssim 1500$ [18]. These were first noticed in WMAP data [19–21] and have persisted [22,23]. None of the

*shinjinibasu@ufl.edu
†daniel.brooker@nrl.navy.mil
‡tsamis@physics.uoc.gr
§woodard@phys.ufl.edu

observed features reaches the 5σ level of a detection, but it is conceivable that this threshold might be reached by correlating them with other data sets [24]. We have suggested the possibility of doing this (in the far future) with data from the tensor power spectrum [25,26]. Here we study the prospects for exploiting non-Gaussianity.

Maldacena's analysis [27] established that single-scalar inflation (1) cannot produce a detectable level of non-Gaussianity if the potential is smooth like (5). The effect from a smooth potential is widely distributed over the angular bispectrum so the standard estimators average over all possible three-point correlators in order to maximize the signal [28,29]. Planck has not seen a statistically significant indication of non-Gaussianity using any of these standard estimators [30]. On the other hand, it has long been recognized that much stronger transient effects can come from features [31–33]. Because these effects are concentrated at certain angular scales, the standard estimators do not resolve them well. An approximate computation of the effect from the first feature indicated that its non-Gaussian signal is not detectable [31]. We will reexamine this problem using some recently developed improvements in approximating the scalar mode functions [26,34], which unfortunately do not alter the previous conclusion.

This paper consists of five sections, of which this Introduction is the first. Section II is devoted to notation and conventions. The various contributions to non-Gaussianity are listed there, and the one associated with features is identified. In Sec. III we apply our approximation for the scalar mode function to derive an analytic expression for the bispectrum as a functional of the inflationary geometry. Section IV optimizes the parameters for a simple model of the first feature in which the bispectrum can be computed exactly. Our conclusions comprise Sec. V.

II. NOTATION AND CONVENTIONS

Our purpose is to elucidate how quantities depend *functionally* on the geometry of inflation. We employ the Hubble representation [35] using Hubble parameter H and the first slow roll parameter ϵ of the homogeneous, isotropic, and spatially flat background geometry of inflation,

$$ds^2 = -dt^2 + a^2(t) d\vec{x} \cdot d\vec{x} \Rightarrow H \equiv \frac{\dot{a}}{a} > 0,$$
$$\epsilon \equiv -\frac{\dot{H}}{H^2} < 1. \tag{6}$$

It is convenient to regard our time variable as $n \equiv \ln[a(t)/a_i]$, the number of e-foldings from the *beginning* of inflation. If inflation ends after n_e e-foldings, then the more familiar number of e-foldings *until* the end of inflation is $N \equiv n_e - n$. With this time variable $\epsilon(n)$ provides the simplest representation for the geometry of inflation with the Hubble parameter evolved from its initial value H_i,

$$H(n) = H_i \exp\Bigg[-\int_0^n dm \epsilon(m)\Bigg]. \tag{7}$$

We use a prime to denote differentiation with respect to n, as in $\epsilon = -H'/H$.

The key unknown in computing both the scalar power spectrum and the bispectrum is the scalar mode function $v(n,k)$. In our notation its equation, Wronskian normalization, and asymptotically early time form are [36,37]

$$v'' + \left(3 - \epsilon + \frac{\epsilon'}{\epsilon}\right) v' + \frac{k^2 v}{H^2 a^2} = 0,$$
$$v v'^* - v' v^* = \frac{i}{\epsilon H a^3}, \qquad v \rightarrow \frac{\exp[-ik \int_0^n \frac{dm}{Ha}]}{\sqrt{2k\epsilon a^2}}. \tag{8}$$

Let n_k stand for the e-folding of the first horizon crossing, when modes of wave number k obey $k \equiv H(n_k) a(n_k)$. One can see from (8) that the mode function rapidly approaches a constant after this time. The scalar power spectrum is computed by evolving $v(n,k)$ from its early time form to this constant,

$$\Delta^2_{\mathcal{R}}(k) = 4\pi G \times \frac{k^3}{2\pi^2} \times |v(n,k)|^2_{n \gg n_k}. \tag{9}$$

Maldacena's expression for the bispectrum [27] can be expressed as the sum of seven contributions, of which three pairs are usually combined [33]. In our notation the $I = 1, \ldots, 7$ contributions each take the form

$$B_I(k_1,k_2,k_3) = (4\pi G)^2 \mathrm{Re}\Bigg[v(n_e,k_1) v(n_e,k_2) v(n_e,k_3) \times i \int_0^{n_e} dn \epsilon(n) H(n) a^3(n) \times \mathcal{B}^*_I(n,k_1,k_2,k_3)\Bigg]. \tag{10}$$

The four unconjugated $\mathcal{B}_I(n,k_1,k_2,k_3)$ combinations are

$$\mathcal{B}_{1+3} = \epsilon\left[\frac{K^4_{123}}{k_2^2 k_3^2} v_1 v_2' v_3' + \frac{K^4_{231}}{k_3^2 k_1^2} v_1' v_2 v_3' + \frac{K^4_{312}}{k_1^2 k_2^2} v_1' v_2' v_3\right], \tag{11}$$

$$\mathcal{B}_2 = \epsilon\left[\left(\frac{k_1^2 + k_2^2 + k_3^2}{H^2 a^2}\right) v_1 v_2 v_3\right], \tag{12}$$

$$\mathcal{B}_{5+6} = \epsilon^2\left[\frac{K^4}{k_2^2 k_3^2} v_1 v_2' v_3' + \frac{K^4}{k_3^2 k_1^2} v_1' v_2 v_3' + \frac{K^4}{k_1^2 k_2^2} v_1' v_2' v_3\right], \tag{13}$$

$$\mathcal{B}_{4+7} = \frac{\epsilon'}{\epsilon}\left[\left(\frac{k_1^2 + k_2^2 + k_3^2}{H^2 a^2}\right) v_1 v_2 v_3 - v_1 v_2' v_3' - v_1' v_2 v_3' - v_1' v_2' v_3\right], \tag{14}$$

where the fourth order momentum factors in (11) and (13) are

$$K^4_{123} \equiv k_1^2(k_2^2+k_3^2) + 2k_2^2k_3^2 - (k_2^2-k_3^2)^2, \quad (15)$$

$$K^4 \equiv k_1^4 + k_2^4 + k_3^4 - 2k_1^2k_2^2 - 2k_2^2k_3^2 - 2k_3^2k_1^2. \quad (16)$$

Two things are apparent from the initial factors of ϵ in expressions (11)–(14). First, non-Gaussianity is small for smooth potentials such as (5) because ϵ is small and varies slowly. From (3) we see that $\epsilon \sim \frac{1}{16} r_* < 0.0044$, and even the factor of ϵ'/ϵ in (14) is $1 - n_s \sim 0.034$. Second, much larger non-Gaussianity can arise from $\mathcal{B}_{4+7}$ in models with features. In that case ϵ remains small, but ϵ'/ϵ can reach order one over a small range of n.

The mode-dependent factors inside the square brackets of (11)–(14) are also informative when combined with three insights from the mode equation (8):

(1) The mode function $v(n,k)$ is oscillatory and falling off like $1/a$ until it freezes into a constant $V(k)$ (which might be complex) around $n \approx n_k$;
(2) The approach to $V(k)$ has real part $\mathrm{Re}[v(n,k)/V(k)] \sim (k/Ha)^2$; and
(3) The approach has $\mathrm{Im}[v(n,k)/V(k)] \sim -1/2\epsilon Ha^3|V(k)|^2$.

Together with the general form (10), these facts imply that the n integrand for each of the four contributions is oscillatory before the largest of the three wave numbers has experienced horizon crossing and falls off like $1/a^2$ thereafter. This has important consequences for designing estimators to detect non-Gaussianity. When the potential is smooth, both $\epsilon(n)$ and $\partial_n \ln[\epsilon]$ are nearly constant, so all wave numbers will show nearly the same effect and the best strategy is to combine them as the standard estimators do. However, when a feature is present, the factor of $\partial_n \ln[\epsilon(n)]$ in (14) becomes significant in a small range of n, and the non-Gaussian signal will be much larger for modes that experience horizon crossing around that time. Averaging over all observable wave numbers runs the risk of drowning a real signal in noise.

Because conventions differ we close by reviewing how the fundamental fields relate to $\Delta^2_{\mathcal{R}}(k)$ and $B(k_1,k_2,k_3)$. We use the gauge of Salopek, Bond, and Bardeen [38] in which time is fixed by setting the inflaton to its background value and the graviton field is transverse. In this gauge the metric components g_{00} and g_{0i} are constrained and the dynamical variables $\zeta(n,\vec{x})$ and $h_{ij}(n,\vec{x})$ reside in the spatial components,

$$g_{ij}(n,\vec{x}) = a^2 e^{2\zeta(n,\vec{x})} \times [e^{h(n,\vec{x})}]_{ij}, h_{ii}(n,\vec{x}) = 0. \quad (17)$$

Scalar perturbations derive from $\zeta(n,\vec{x})$ whose free field expansion is

$$\tilde{\zeta}(n,\vec{k}) \equiv \int d^3x e^{-i\vec{k}\cdot\vec{x}} \zeta(n,\vec{x}) = \sqrt{4\pi G}\Big[v(n,k)\alpha(\vec{k}) + v^*(n,k)\alpha^\dagger(-\vec{k})\Big], \quad (18)$$

where $\alpha^\dagger$ and α are creation and annihilation operators,

$$[\alpha(\vec{k}), \alpha^\dagger(\vec{p})] = (2\pi)^3\delta^3(\vec{k}-\vec{p}), \qquad \alpha(\vec{k})|\Omega\rangle = 0. \quad (19)$$

Assuming the wave numbers experience horizon crossing before the end of inflation n_e, our power spectrum and bispectrum are

$$\langle\Omega|\tilde{\zeta}(n_e,\vec{k})\tilde{\zeta}(n_e,\vec{p})|\Omega\rangle = \frac{2\pi^2}{k^3} \times \Delta^2_{\mathcal{R}}(k) \times (2\pi)^3\delta^3(\vec{k}+\vec{p}), \quad (20)$$

$$\langle\Omega|\tilde{\zeta}(n_e,\vec{k}_1)\tilde{\zeta}(n_e,\vec{k}_2)\tilde{\zeta}(n_e,\vec{k}_3)|\Omega\rangle = B(k_1,k_2,k_3) \times (2\pi)^3\delta^3(\vec{k}_1+\vec{k}_2+\vec{k}_3). \quad (21)$$

Note that while the power spectrum is dimensionless, the bispectrum has the dimension of k^6.

III. ANALYTIC APPROXIMATION FOR THE BISPECTRUM

In this section we first convert the key contribution (14) from the mode function $v(n,k)$ to its norm square $N(n,k)$. Then we introduce an approximation [26,34] that should be very accurate for the physically relevant case of small $\epsilon(n)$ but significant $\partial_n \ln[\epsilon(n)]$. Finally, we study a model of the first feature to compare our result for $B_{4+7}(k_1,k_2,k_3)$ with the simpler approximation of Adshead, Hu, Dvorkin, and Peiris [31].

A. Approximating the mode functions

Even considered as a purely numerical problem, it is better to convert Eqs. (8) for $v(n,k)$ into relations for $N(n,k) \equiv |v(n,k)|^2$ [39]. Avoiding the need to keep track of the phase makes about a quadratic improvement in convergence. Further, nothing is lost because the phase can be recovered by a simple integration [26],

$$v(n,k) = \sqrt{N(n,k)}\exp\left[-i\int_0^n \frac{dm}{2\epsilon Ha^3 N}\right] \equiv \sqrt{N(n,k)}e^{i\theta(n,k)}. \quad (22)$$

It is best to begin with the outer factors of $v(n_e,k)$ in expression (10). Assuming the various wave numbers have experienced horizon crossing, these outer mode functions can be expressed in terms of the power spectrum (9),

$$v(n_e,k) = \sqrt{\frac{\pi}{2Gk^3}}\Delta_{\mathcal{R}}(k)e^{i\theta(n_e,k)}. \quad (23)$$

We next combine each outer phase with the appropriate inner phase,

$$\hat{v}(n,k) \equiv v(n,k)e^{-i\theta(n_e,k)} \Rightarrow \theta(n,k) - \theta(n_e,k) = \int_n^{n_e} \frac{dm}{\epsilon H a^3 N} \equiv \phi(n,k). \quad (24)$$

Note that $\phi(n,k)$ approaches zero like $1/a^3$ for large n. At this stage one can recognize the real part of the undifferentiated terms,

$$\mathrm{Re}[i\hat{v}_1^*\hat{v}_2^*\hat{v}_3^*] = \sqrt{N_1N_2N_3}\sin(\phi_1+\phi_2+\phi_3). \quad (25)$$

The differentiated terms are more complicated,

$$\hat{v}'(n,k) = \hat{v}(n,k)\left[\frac{N'(n,k)}{2N(n,k)} + i\phi'(n,k)\right]. \quad (26)$$

Hence we have

$$\mathrm{Re}[i\hat{v}_1^*\hat{v}_2'^*\hat{v}_3'^*] = \sqrt{N_1N_2N_3}\left\{\sin(\phi_1+\phi_2+\phi_3)\left[\frac{N_2'}{2N_2}\frac{N_3'}{2N_3} - \phi_2'\phi_3'\right] + \cos(\phi_1+\phi_2+\phi_3)\left[\frac{N_2'}{2N_2}\phi_3' + \frac{N_3'}{2N_3}\phi_2'\right]\right\}. \quad (27)$$

There are three terms such as (27), so putting everything together gives

$$B_{4+7}(k_1,k_2,k_3) = \frac{4\pi^4\Delta_{\mathcal{R}}(k_1)\Delta_{\mathcal{R}}(k_2)\Delta_{\mathcal{R}}(k_3)}{k_1^2k_2^2k_3^2} \times \sqrt{\frac{2Gk_1k_2k_3}{\pi}}\int_0^{n_e} dn\epsilon' H a^3 \times \sqrt{N_1N_2N_3}\left\{\sin(\phi_1+\phi_2+\phi_3)\left[\left(\frac{k_1^2+k_2^2+k_3^2}{H^2a^2}\right) - \frac{N_2'}{2N_2}\frac{N_3'}{2N_3} + \phi_2'\phi_3' - \cdots\right] - \cos(\phi_1+\phi_2+\phi_3)\left[\frac{N_1'}{2N_1}(\phi_2'+\phi_3') + \frac{N_2'}{2N_2}(\phi_3'+\phi_1') + \frac{N_3'}{2N_3}(\phi_1'+\phi_2')\right]\right\}. \quad (28)$$

To develop a useful approximation for (28) we first factor $N(n,k)$ into the instantaneously constant ϵ solution $N_0(n,k)$ times the exponential of a residual $g(n,k)$, which is sourced by derivatives of $\ln[\epsilon(n)]$ [26,34],

$$N(n,k) = N_0(n,k) \times \exp\left[-\frac{1}{2}g(n,k)\right]. \quad (29)$$

Of course, the derivatives of $\ln[\epsilon(n)]$ that source $g(n,k)$ are of great concern in the study of features, as is the potentially large factor of $1/\epsilon$ in $N_0(n,k)$. Taking all the other factors of ϵ to zero causes a negligible loss of accuracy. The resulting approximation involves three functions $\tilde{g}(n,n_k)$, $\tilde{\gamma}'(n,n_k)$, and $\tilde{\phi}(n,n_k)$, which must be tabulated over a narrow range of n and n_k,

$$\tilde{B}_{4+7}(k_1,k_2,k_3) = \frac{4\pi^4\Delta_{\mathcal{R}}(k_1)\Delta_{\mathcal{R}}(k_2)\Delta_{\mathcal{R}}(k_3)}{k_1^2k_2^2k_3^2} \times -\int_0^{n_e} dn\partial_n\sqrt{\frac{GH^2(n)}{\pi\epsilon(n)}} \times \sqrt{(1+e^{2\Delta n_1})(1+e^{2\Delta n_2})(1+e^{2\Delta n_3})}e^{-\frac{1}{2}(\tilde{g}_1+\tilde{g}_2+\tilde{g}_3)}\left\{\sin(\tilde{\phi}_1+\tilde{\phi}_2+\tilde{\phi}_3) \times \left[e^{-2\Delta n_1} - \left(\frac{1}{1+e^{2\Delta n_2}}+\frac{1}{4}\tilde{\gamma}_2'\right)\left(\frac{1}{1+e^{2\Delta n_3}}+\frac{1}{4}\tilde{\gamma}_3'\right) + \tilde{\phi}_2'\tilde{\phi}_3' + (231) + (312)\right] - \cos(\tilde{\phi}_1+\tilde{\phi}_2+\tilde{\phi}_3)\left[\left(\frac{1}{1+e^{2\Delta n_1}}+\frac{1}{4}\tilde{\gamma}_1'\right)(\tilde{\phi}_2'+\tilde{\phi}_3') + (231) + (312)\right]\right\}. \quad (30)$$

Here and henceforth $\Delta n_i \equiv n - n_i$, where n_i is the e-folding at which wave number k_i experiences horizon crossing.

The tabulated function $\tilde{g}(n,n_k)$ represents an approximation of the amplitude residual $g(n,k)$ in (29). It is expressed as Green's function integral over sources before and after horizon crossing,

$$S_b(m) = \partial_m^2\ln[\epsilon(m)] + \frac{1}{2}(\partial_m\ln[\epsilon(m)])^2 + 3\partial_m\ln[\epsilon(m)], \quad (31)$$

$$S_a(m,n_k) = \frac{2\partial_m\ln[\epsilon(m)]}{1+e^{2\Delta m}} + \left(\frac{2e^{-\Delta m}\frac{\epsilon(n_k)}{\epsilon(m)}}{1+e^{2\Delta m}}\right)^2, \quad (32)$$

where $\Delta m \equiv m - n_k$. The integral expression for $\tilde{g}(n, n_k)$ is

$$\tilde{g}(n, n_k) = -2\theta(-\Delta n) \int_0^n dm G(\Delta m, \Delta n) S_b(m) + 2\theta(\Delta n) \Bigg\{ G(0, \Delta n) \frac{\epsilon'(n_k)}{\epsilon(n_k)} - \int_0^{n_k} dm G(\Delta m, \Delta n) S_b(m) - \int_{n_k}^n dm G(\Delta m, \Delta n) S_a(m, n_k) \Bigg\}, \tag{33}$$

where Green's function is

$$G(\Delta m, \Delta n) = \frac{1}{2}(e^{\Delta m} + e^{3\Delta m}) \times \sin[2e^{-\Delta m} - 2\tan^{-1}(e^{-\Delta m}) - 2e^{-\Delta n} + 2\tan^{-1}(e^{-\Delta n})]. \tag{34}$$

Differentiating the Green's function with respect to n gives

$$\partial_n G(\Delta m, \Delta n) = \left(\frac{e^{\Delta m} + e^{3\Delta m}}{e^{\Delta n} + e^{3\Delta n}} \right) \times \cos[2e^{-\Delta m} - 2\tan^{-1}(e^{-\Delta m}) - 2e^{-\Delta n} + 2\tan^{-1}(e^{-\Delta n})]. \tag{35}$$

It occurs in the second of the tabulated functions,

$$\tilde{\gamma}'(n, n_k) = 2\theta(-\Delta n) \partial_n \ln[\epsilon(n)] + \partial_n \tilde{g}(n, n_k). \tag{36}$$

The final tabulated function is our approximation of the angle $\phi(n, k)$,

$$\tilde{\phi}(n, n_k) = \int_n^{n_e} dm \frac{e^{-\Delta m + \frac{1}{2}\tilde{g}(m, n_k)}}{1 + e^{2\Delta m}}. \tag{37}$$

Note that its derivative does not require separate tabulation,

$$\tilde{\phi}'(n, n_k) = -\frac{e^{-\Delta n + \frac{1}{2}\tilde{g}(n, n_k)}}{1 + e^{2\Delta n}}. \tag{38}$$

Adshead, Hu, Dvorkin, and Peiris [31] introduced a much simpler approximation that, in our language, corresponds to setting $\tilde{g}(n, n_k)$ and $\tilde{\gamma}'(n, k)$ to zero in expression (30). Note that this reduces the angle and its derivative to be functions of just the single variable $\Delta n = n - n_k$,

$$\tilde{\phi}(n, n_k)\Big|_{\tilde{g}=0} = e^{-\Delta n} - \tan^{-1}(e^{-\Delta n}),$$
$$\tilde{\phi}'(n, n_k)\Big|_{\tilde{g}=0} = -\frac{e^{-\Delta n}}{1 + e^{2\Delta n}}. \tag{39}$$

This approximation is certainly simpler to implement, but it completely ignores how the inner mode functions change in response to the feature.

B. The step model

The model we shall study belongs to a class introduced in 2001 by Adams, Cresswell, and Easther [40],

$$V(\varphi) = \frac{1}{2} m^2 \varphi^2 \times \left[1 + c \tanh\left(\frac{\varphi - b}{d} \right) \right]. \tag{40}$$

A fit to the first feature ($20 \lesssim \ell \lesssim 40$) using WMAP data gave [41]

$$b = \frac{14.668}{\sqrt{8\pi G}}, \qquad c = 1.505 \times 10^{-3},$$
$$d = \frac{0.02705}{\sqrt{8\pi G}}, \qquad m = \frac{7.126 \times 10^{-6}}{\sqrt{8\pi G}}. \tag{41}$$

Figure 1 shows the first slow roll parameter and its logarithmic derivative for this model. Two obvious points are the following:

(1) The first slow roll parameter is always very small;[1] and
(2) The crucial factor of $\partial_n \ln[\epsilon(n)]$ that sources non-Gaussianity is only significant for the two e-foldings $170.8 \lesssim n \lesssim 172.8$.

Inflation ends for this model at $n_e \simeq 225.6$ so the feature peaks about 54 e-foldings before the end of inflation.

Let us first establish that our approximations for the amplitude correction (33) and for the phase (37) are valid. Figure 2 displays the exact results (in blue) versus our approximations (in yellow) for the case of $n_k = 172.5$ where the amplitude correction is close to its maximum. The agreement is good, except for an offset at late times that is due to $g(n, k)$ having become large enough around $n \approx 172$ that nonlinear corrections matter [34]. For most values of n_k this is not an issue and, even for $n_k = 172.5$, the rightmost graph of Fig. 1 shows that the offset has little effect on non-Gaussianity.

In view of point 2 above, we only require the tabulated functions $\tilde{g}(n, n_k)$, $\tilde{\gamma}'(n, n_k)$, and $\tilde{\phi}(n, nk)$ for the two e-foldings from $n = 170.8$ to $n = 172.8$. Figure 3 shows contour plots of these functions for modes that experience horizon crossing in the range $170 < n_k < 173.5$. It is important to bear in mind that the source $\partial_n \ln[\epsilon(n)]$ in Fig. 1 modulates how the corrections of Fig. 3 affect non-Gaussianity. So although the graph of $\tilde{g}(n, n_k)$ shows a strong amplitude enhancement for $n_k \simeq 171.5$, and an equally strong suppression for $n_k \simeq 172.5$, the latter effect

[1] It is actually a little too large for the improved bounds on the tensor-to-scalar ratio [6] since the time of WMAP. However, the model serves well enough for the purposes of illustration.

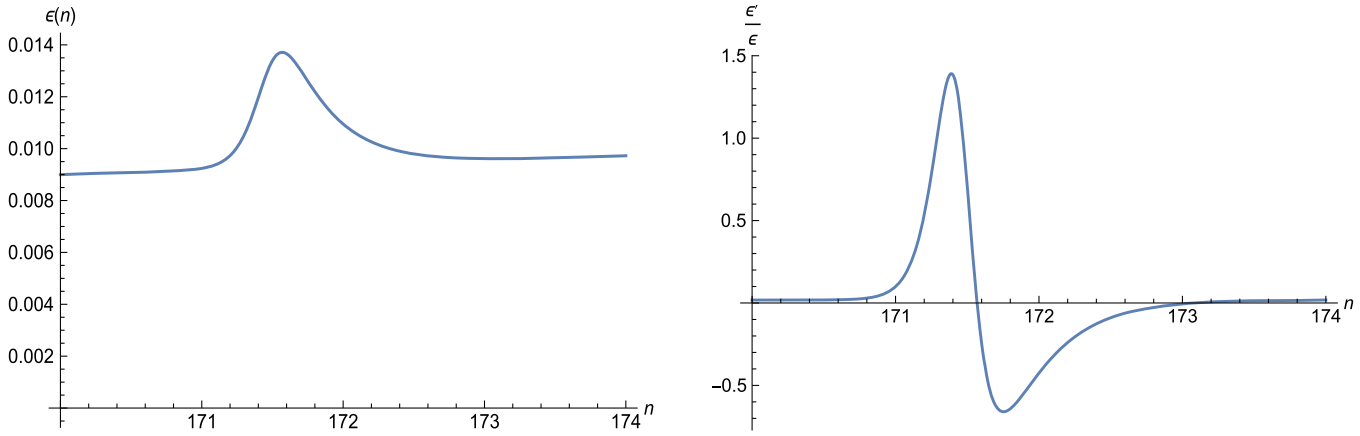

FIG. 1. The left-hand graph gives $\epsilon(n)$ for the step model (40)–(41). The right-hand graph shows $\partial_n \ln[\epsilon(n)]$ for this model. Note that the logarithmic derivative is only significant in the narrow range $170.8 \lesssim n \lesssim 172.8$.

is much less significant because it peaks for $n \gtrsim 172.1$, by which point $\partial_n \ln[\epsilon(n)]$ is small. Because of this modulation, the biggest correction comes from the large positive phase shift at $n_k \simeq 172.6$, which peaks at $n \simeq 171.7$.

Figure 4 gives some idea of the significance of the various corrections we have introduced to the approximation of Adshead, Hu, Dvorkin, and Peiris [31], but it is limited by the assumption that $k_1 = k_2 = k_3$. The

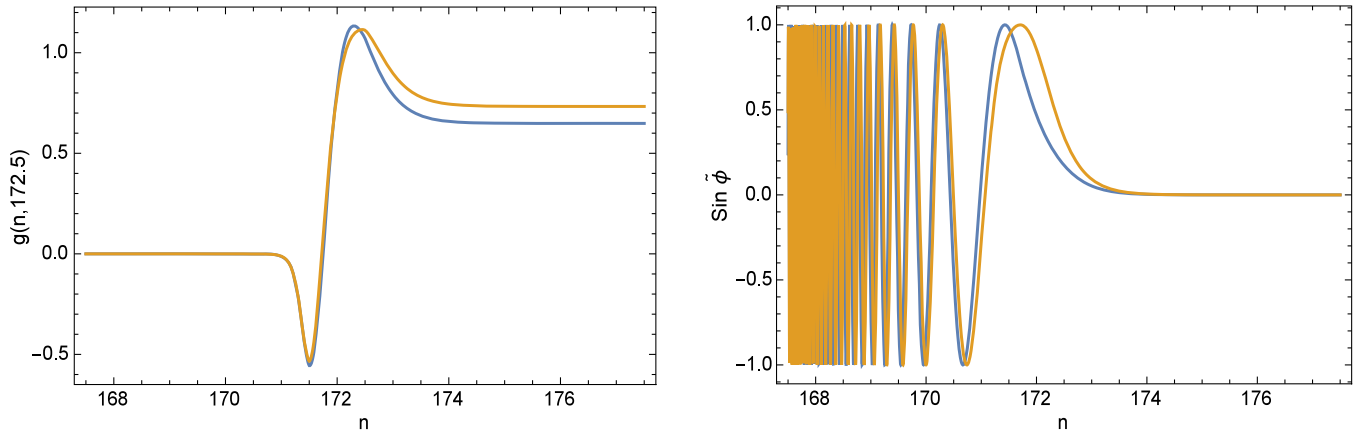

FIG. 2. Comparison between exact results (in blue) and our approximations (in yellow) for the amplitude correction (33) and the phase (37). The left-hand graph shows $g(n,k)$ and the right-hand graph shows $\sin[\tilde{\phi}(n,k)]$.

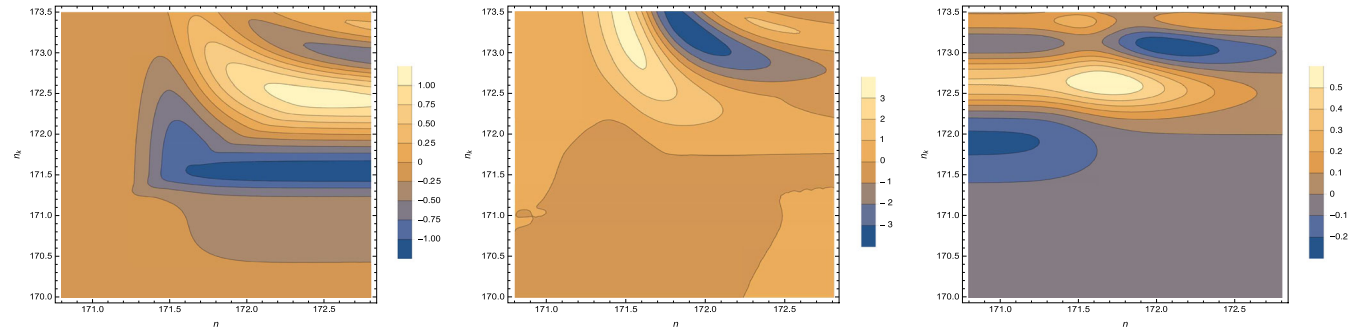

FIG. 3. Various correction factors for the step model. The left-hand graph gives our approximation (33) for (−4 times the logarithm of) the amplitude correction $g(n,n_k)$ in the step model. The middle graph shows the derivative factor (36). And the right-hand graph shows how much our approximation (37) differs from the de Sitter result (39).

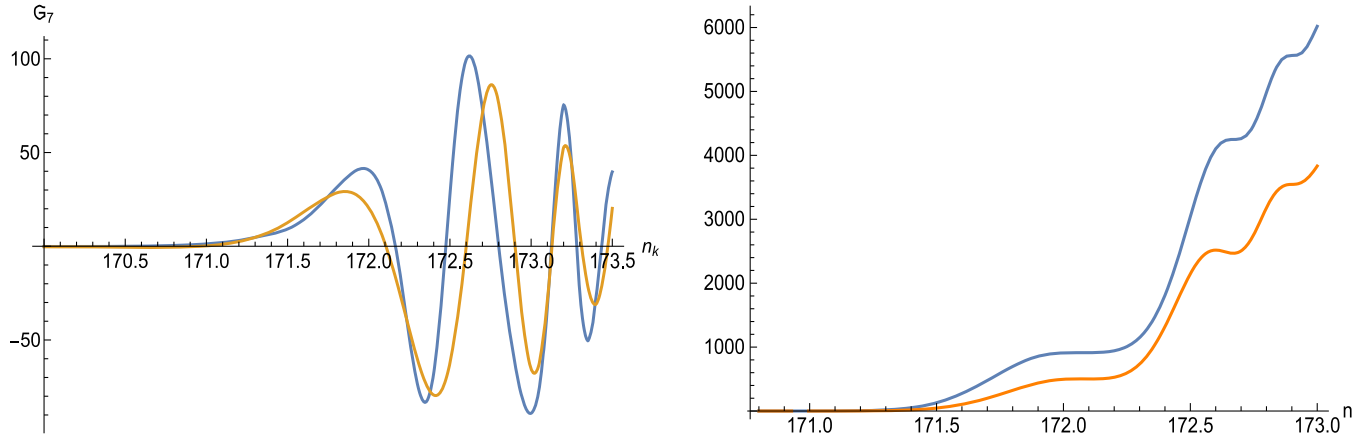

FIG. 4. The left-hand graph shows the "inner" part of expression (30), starting from $-\int_0^{n_\epsilon} dn\ldots$, for the equilateral triangle case of $k_1 = k_2 = k_3$. The blue curve shows our approximation while the yellow curve shows the simpler approximation of Adshead, Hu, Dvorkin, and Peiris [31]. The right-hand graph shows the integral of the square of our approximation (in blue) versus the product of our approximation times theirs (in yellow). The ratio of the areas under the yellow to the blue curves is about 0.637 at the end.

correlators Hung, Fergusson, and Shellard [42] provide a more detailed comparison between any two bispectra $B_i(k_1, k_2, k_3)$ and $B_j(k_1, k_2, k_3)$ that possess the same power spectrum $\Delta^2_{\mathcal{R}}(k)$. They are formed from ratios of "inner products" defined as

$$[B_i, B_j] \equiv \text{const} \times \int_{\mathcal{V}_B} dk_1 dk_2 dk_3 (k_1 k_2 k_3)^4 \times \frac{B_i(k_1, k_2, k_3) B_j(k_1, k_2, k_3)}{\Delta^2_{\mathcal{R}}(k_1)\Delta^2_{\mathcal{R}}(k_2)\Delta^3_{\mathcal{R}}(k_3)}, \tag{42}$$

where $\mathcal{V}_B$ indicates the range of the wave numbers that obey the triangle condition ($|k_1 - k_2| < k_3 < k_1 + k_2$), plus whatever other restrictions we wish to impose, and the multiplicative constant is irrelevant. Hung, Fergusson, and Shellard use these inner products to form, respectively, shape, amplitude, and total correlators,

$$\mathcal{S}(B_i, B_j) \equiv \frac{[B_i, B_j]}{\sqrt{[B_i, B_i][B_j, B_j]}}, \quad \mathcal{A}(B_i, B_j) \equiv \sqrt{\frac{[B_i, B_i]}{[B_j, B_j]}}, \tag{43}$$

$$\mathcal{T}(B_i, B_j) \equiv 1 - \sqrt{\frac{[B_j - B_i, B_j - B_i]}{[B_j, B_j]}}. \tag{44}$$

We evaluated all three correlators to compare our approximation (as B_i) with the simpler approximation (as B_j) of Adshead, Hu, Dvorkin, and Peiris [31] over the narrow range $170.8 < n_i < 173$ of the greatest response. The results are

$$\mathcal{S} \simeq 0.9578, \qquad \mathcal{A} \simeq 1.3436, \qquad \mathcal{T} \simeq 0.5189. \tag{45}$$

Even though the equilateral triangle case shown by Fig. 4 seems to roughly agree we can see there is quite a large mismatch in the amplitudes that leads to a substantial degradation of the total correlator.

IV. THE SQUARE WELL MODEL

In 1992 Starobinsky proposed a simple model in which the first slow roll parameter makes an instantaneous jump from one value to another, which permits the mode functions to be solved exactly [43]. Because the fundamental source of non-Gaussianity $\partial_n \ln[\epsilon(n)]$ is a delta function for this case, one can exactly compute $B_{4+7}(k_1, k_2, k_3)$ and derive excellent approximations for the remaining contributions [44–46]. We shall make a slight modification of this model in which $\epsilon(n)$ returns to its original value after a short number of e-foldings Δn,

$$\epsilon(n) = \epsilon_1 \theta(n_0 - n) + \epsilon_2 \theta(n - n_0)\theta(n_0 + \Delta n - n) + \epsilon_1 \theta(n - n_0 - \Delta n). \tag{46}$$

We first solve exactly for the mode functions. Next a determination is made of the parameter values for n_0, Δn, ϵ_1, and ϵ_2 to cause the scalar power spectrum of this model to agree with a numerical determination of the step model power spectrum of Sec. III. B over the crucial range $170.8 < n_k < 172.8$. After doing that $B_{4+7}(k_1, k_2, k_3)$ is computed exactly, and then in the approximation of setting all small factors of ϵ to zero. We close by using the correlators (43) and (44) of Hung, Fergusson, and Shellard [42] to compare this exactly solvable model with our approximation and with the simpler approximation of Adshead, Hu, Dvorkin, and Peiris [31].

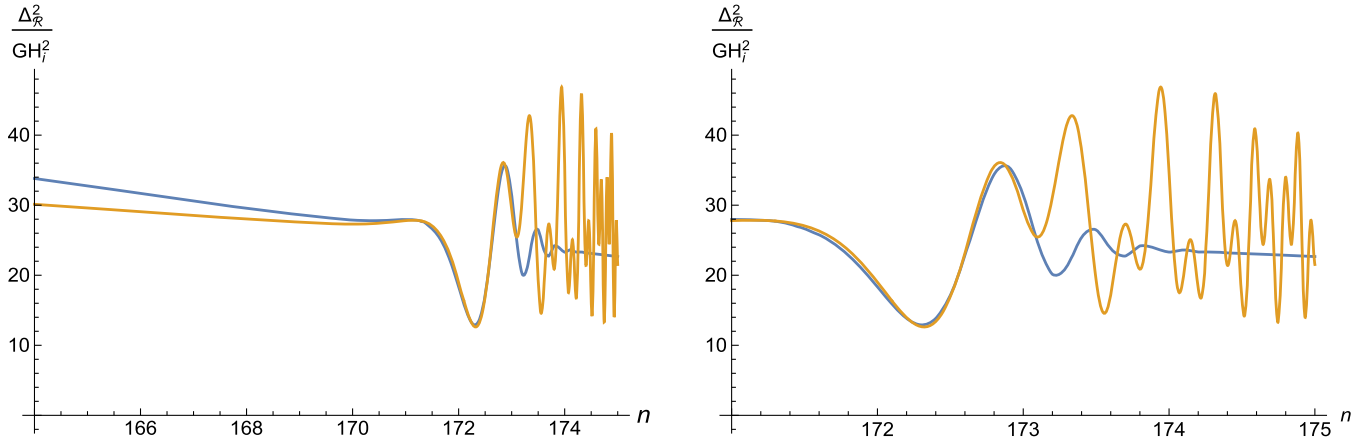

FIG. 5. Both graphs show the $\Delta^2_{\mathcal{R}}(k)$ as a function of e-folding of horizon crossing, for the step model (in blue) and for the best fit square well model (in yellow). The approximate conversion to the wave number is $k \simeq a_i m e^n \sqrt{150 - \frac{2}{3}n}$, where a_i is the scale factor at the beginning of inflation and $m = 7.126 \times 10^{-6}\sqrt{8\pi G}$.

For $\epsilon(n) = \epsilon_i$ for all time then the exact mode function is

$$v_i(n,k) = \sqrt{\frac{\pi}{4\epsilon_i(1-\epsilon_i)Ha^3}} H^{(1)}_{\nu_i}\left(\frac{k}{(1-\epsilon_i)Ha}\right),$$
$$\nu_i = \frac{1}{2}\left(\frac{3-\epsilon_i}{1-\epsilon_i}\right). \tag{47}$$

For the actual parameter (46) the mode function takes the form,

$$v(n,k) = v_1(n,k)\theta(n_0 - n) + v_B(n,k)\theta(n-n_0)\theta(n_0+\Delta n - n) + v_C(n,k)\theta(n-n_0-\Delta n), \tag{48}$$

where $v_B(n,k)$ and $v_C(n,k)$ are,

$$v_B(n,k) = \alpha v_2(n,k) + \beta v_2^*(n,k), \tag{49}$$

$$v_C(n,k) = \alpha[\gamma v_1(n,k) + \delta v_1^*(n,k)] + \beta[\gamma v_1(n,k) + \delta v_1^*(n,k)]^*. \tag{50}$$

The appropriate matching conditions at $n = n_0$ and $n = n_0 + \Delta n$ are the continuity of $v(n,k)$ and of the product $\epsilon(n) \times v'(n,k)$. The coefficients α and β involve the mode functions (47) and their derivatives evaluated at $n = n_0$,

$$\alpha = -iHa^3[\epsilon_2 v_1 v_2^{*\prime} - \epsilon_1 v_1' v_2^*],$$
$$\beta = iHa^3[\epsilon_2 v_1 v_2' - \epsilon_1 v_1' v_2]. \tag{51}$$

The coefficients γ and δ involve the mode functions (47) and their derivatives evaluated at $n = n_0 + \Delta n$,

$$\gamma = -iHa^3[\epsilon_1 v_2 v_1^{*\prime} - \epsilon_2 v_2' v_1^*],$$
$$\delta = iHa^3[\epsilon_1 v_2 v_1' - \epsilon_2 v_2' v_1]. \tag{52}$$

From expression (50) and the small argument form of the Hankel function we infer the late time limit of the mode function,

$$\lim_{n \gg n_k} v_C(n,k) = -\frac{iH(n_k)}{\sqrt{2\epsilon_1 k^3}} \times \frac{\Gamma(\nu_1)[2(1-\epsilon_1)]^{\frac{1}{1-\epsilon_1}}}{\sqrt{\pi}} \times [\alpha(\gamma-\delta) - \beta(\gamma^* - \delta^*)]. \tag{53}$$

Substituting this in expression (9) gives the square well model's prediction for the scalar power spectrum,

$$\Delta^2_{\mathcal{R}}(k) = \frac{GH^2(n_k)}{\pi\epsilon_1} \times \frac{\Gamma^2(\nu_1)[2(1-\epsilon_1)]^{\frac{2}{1-\epsilon_1}}}{\pi} \times |\alpha(\gamma-\delta) - \beta(\gamma^* - \delta^*)|^2. \tag{54}$$

Figure 5 compares (54) with a numerical determination of $\Delta^2_{\mathcal{R}}(k)$ for the step model. There is no way to make the two results agree for all values of n_k; however, very good concurrence over the key range of $170.8 < n_k < 172.8$ results from the following choices for the square well parameters,

$$n_0 = 171.3, \quad \Delta n = 0.7, \quad \epsilon_1 = 0.0093, \quad \epsilon_2 = 0.0137. \tag{55}$$

The infinite sequence of oscillations ("ringing") evident in Fig. 5 is the result of the sharp transitions in $\epsilon(n)$ for the square well model (46). For smooth transitions, such as those of the step model, the oscillations decay rapidly.

Of course, no one understands what caused features (if they are present) so it may be that the transition really *is* instantaneous, in which case ringing is a prominent signature that persists long after the transition. This possibility was pursued in a fascinating study by Adshead, Dvorkin, Hu, and Lim [32]. However, we shall here take the view that ringing is an artifact of modeling smooth transitions as instantaneous, and we shall accordingly focus narrowly on the two e-foldings $170.8 < n_k < 172.8$ over which the square well model is in reasonable agreement with the step model.

The great advantage of the square well model is that the key modulation factor of ϵ'/ϵ in expression (14) is a delta function,

$$\frac{\epsilon'(n)}{\epsilon(n)} = \ln\left(\frac{\epsilon_2}{\epsilon_1}\right)[\delta(n-n_0) - \delta(n-n_1)], \tag{56}$$

where $n_1 \equiv n_0 + \Delta n$. We must also understand how to evaluate certain discontinuous factors at the jumps,

$$\epsilon(n_0) \longrightarrow \left(\frac{\epsilon_1+\epsilon_2}{2}\right) \leftarrow \epsilon(n_1), \tag{57}$$

$$\epsilon(n_0)v'(n_0,k_\alpha)v'(n_0,k_\beta) \longrightarrow \left(\frac{\epsilon_1+\epsilon_2}{2}\right)\frac{\epsilon_1}{\epsilon_2}v_1'(n_0,k_\alpha)v_1'(n_0,k_\beta), \tag{58}$$

$$\epsilon(n_1)v'(n_1,k_\alpha)v'(n_1,k_\beta) \longrightarrow \left(\frac{\epsilon_1+\epsilon_2}{2}\right)\frac{\epsilon_2}{\epsilon_1}v_B'(n_1,k_\alpha)v_B'(n_1,k_\beta). \tag{59}$$

Substituting relations (56) and (57)–(59) into expressions (10) and (14) gives

$$B_{4+7}(k_1,k_2,k_3) = (4\pi G)^2\left(\frac{\epsilon_1+\epsilon_2}{2}\right)\ln\left(\frac{\epsilon_2}{\epsilon_1}\right)\mathrm{Re}[iv_C(n_e,k_1)v_C(n_e,k_2)v_C(n_e,k_3) \times [H(n_0)a^3(n_0)F^*(n_0,k_1,k_2,k_3) - H(n_1)a^3(n_1)G^*(n_1,k_1,k_2,k_3)]], \tag{60}$$

where the upper and lower factors are

$$F(n,k_1,k_2,k_3) \equiv \frac{(k_1^2+k_2^2+k_3^2)}{H^2(n)a^2(n)}v_1(n,k_1)v_1(n,k_2)v_1(n,k_3) - \frac{\epsilon_1}{\epsilon_2}v_1(n,k_1)v_1'(n,k_2)v_1'(n,k_3) - \frac{\epsilon_1}{\epsilon_2}v_1'(n,k_1)v_1(n,k_2)v_1'(n,k_3) - \frac{\epsilon_1}{\epsilon_2}v_1'(n,k_1)v_1'(n,k_2)v_1(n,k_3), \tag{61}$$

$$G(n,k_1,k_2,k_3) \equiv \frac{(k_1^2+k_2^2+k_3^2)}{H^2(n)a^2(n)}v_B(n,k_1)v_B(n,k_2)v_B(n,k_3) - \frac{\epsilon_2}{\epsilon_1}v_B(n,k_1)v_B'(n,k_2)v_B'(n,k_3) - \frac{\epsilon_2}{\epsilon_1}v_B'(n,k_1)v_B(n,k_2)v_B'(n,k_3) - \frac{\epsilon_2}{\epsilon_1}v_B'(n,k_1)v_B'(n,k_2)v_B(n,k_3). \tag{62}$$

Expressions (60)–(62) are exact, but somewhat opaque because they conceal certain large factors of $1/\epsilon$, and because they are obscured by many other negligibly small positive powers of ϵ. There is no appreciable loss of accuracy, and a considerable simplification, by extracting the large factors of $1/\epsilon$ and setting the other factors of ϵ to zero. Note that this makes the Hubble parameter constant. Two ratios that involve the momenta are

$$\kappa_i \equiv \frac{k_i}{H(n_0)a(n_0)} \to e^{n_{k_i}-n_0},$$
$$\lambda_i \equiv \frac{k_i}{H(n_1)a(n_1)} \to e^{n_{k_i}-n_1} = \kappa_i e^{-\Delta n}. \tag{63}$$

Applying these approximations to the mode functions (at n_0 and n_1) and their first derivatives gives

$$v_i(n_0,k) \to -\frac{iH(1-i\kappa)e^{i\kappa}}{\sqrt{2\epsilon_i k^3}}, \quad v_i'(n_0,k) \to \frac{iH\kappa^2 e^{i\kappa}}{\sqrt{2\epsilon_1 k^3}}, \tag{64}$$

$$v_i(n_1,k) \to -\frac{iH(1-i\lambda)e^{i\lambda}}{\sqrt{2\epsilon_i k^3}}, \quad v_i'(n_1,k) \to \frac{iH\lambda^2 e^{i\lambda}}{\sqrt{2\epsilon_i k^3}}. \tag{65}$$

These approximations carry the first set of combination coefficients (51) to

$$\alpha_i \to \frac{i}{2\kappa_i}\left[(1-i\kappa_i)\sqrt{\frac{\epsilon_2}{\epsilon_1}} - (1+i\kappa_i)\sqrt{\frac{\epsilon_1}{\epsilon_2}}\right], \tag{66}$$

$$\beta_i \to \frac{i}{2\kappa_i}(1-i\kappa_i)\left[\sqrt{\frac{\epsilon_2}{\epsilon_1}} - \sqrt{\frac{\epsilon_1}{\epsilon_2}}\right]e^{2i\kappa_i}. \tag{67}$$

Only the difference of the second set (52) matters, and it becomes

$$\gamma_i - \delta_i \to \frac{e^{i\lambda_i}}{\lambda_i}\left[(1-i\lambda_i)\sin(\lambda_i)\sqrt{\frac{\epsilon_1}{\epsilon_2}} - \left[\sin(\lambda_i) - \lambda_i\cos(\lambda_i)\right]\sqrt{\frac{\epsilon_2}{\epsilon_1}}\right]. \quad (68)$$

With these approximations expression (14) assumes the form

$$B_{4+7}(k_1,k_2,k_3) \to \frac{(\pi GH^2)^2}{k_1^2k_2^2k_3^2}\left(\frac{\epsilon_1+\epsilon_2}{\epsilon_1^3}\right)\ln\left(\frac{\epsilon_2}{\epsilon_1}\right)\mathrm{Re}\left[\frac{iA_1A_2A_3}{\kappa_1\kappa_2\kappa_3} \times \left[\mathcal{F}^* e^{-i(\kappa_1+\kappa_2+\kappa_3)} - \left(\frac{\epsilon_1}{\epsilon_2}\right)^{\frac{3}{2}}\mathcal{G}^* e^{-i(\lambda_1+\lambda_2+\lambda_3)}\right]\right], \quad (69)$$

where $A_i \equiv \alpha_i(\gamma_i - \delta_i) - \beta_i(\gamma_i^* - \delta_i^*)$ and the approximated factors are

$$\mathcal{F} = (\kappa_1^2+\kappa_2^2+\kappa_3^2)(1-i\kappa_1)(1-i\kappa_2)(1-i\kappa_3) - \frac{\epsilon_1}{\epsilon_2}\kappa_1^2\kappa_2^2(1-i\kappa_3) - \frac{\epsilon_1}{\epsilon_2}\kappa_1^2\kappa_3^2(1-i\kappa_2) - \frac{\epsilon_1}{\epsilon_2}\kappa_2^2\kappa_3^2(1-i\kappa_1), \quad (70)$$

$$\mathcal{G} = e^{\Delta n}(\kappa_1^2+\kappa_2^2+\kappa_3^2)\prod_{i=1}^{3}[\alpha_i(1-i\lambda_i) - \beta_i(1+i\lambda_i)e^{-2i\lambda_i}] - e^{-\Delta n}\frac{\epsilon_2}{\epsilon_1}\sum_{i=1}^{3}\left[\prod_{j\neq i}\kappa_j^2(\alpha_j - \beta_j e^{-2i\lambda_j})\right] \times [\alpha_i(1-i\lambda_i) - \beta_i(1+i\lambda_i)e^{-2i\lambda_i}]. \quad (71)$$

One can see from Fig. 5 that the power spectra of the square well model and the step model agree almost perfectly over the region $170.8 < n < 173$. This might seem to indicate that they would produce nearly the same non-Gaussian signal, at least when restricted to the same narrow range. However, the results are disappointing when the two models are compared using the shape, amplitude, and total correlators (43)–(44) of Hung, Fergusson, and Shellard [42],

$$\mathcal{S} \simeq 0.7976, \qquad \mathcal{A} \simeq 1.1050, \qquad \mathcal{T} \simeq 0.3230, \quad (72)$$

where B_i was the square well model and B_j was the step model. The amplitudes of the two models are in much better agreement than for the comparison (45) of the step model with the approximation of Adshead, Hu, Dvorkin, and Peiris [31]. However, the shapes disagree, which results in an even lower total correlator. Note that the problem in this case did not arise from inaccurately modeling the non-Gaussian response to a given history $\epsilon(n)$, but rather from the fact that different histories produce different bispectra, even when the power spectra are very similar.

We also compared the square well model (as B_i) with the approximation of Adshead, Hu, Dvorkin, and Peiris [31] (as B_j),

$$\mathcal{S} \simeq 0.8946, \qquad \mathcal{A} \simeq 1.4847, \qquad \mathcal{T} \simeq 0.2598. \quad (73)$$

Both the shape correlator and the amplitude correlator are worse than for the comparison (45) of our approximation with that of Adshead, Dvorkin, Hu, and Peiris, resulting in a much smaller total correlator.

V. EPILOGUE

We have examined the non-Gaussianity associated with conjectured sharp variations in the first slow roll parameter $\epsilon(n)$ known as "features." In Sec. II we identified the crucial contribution, Eq. (14), which becomes significant for features. Section III applied an approximation for how the scalar mode functions depend analytically on $\epsilon(n)$ [26,34] to develop an approximation (30) for this term. Our result involves three tabulated functions of the instantaneous e-folding n and the e-folding of horizon crossing n_k:

(1) $\tilde{g}(n,n_k)$ given in expression (33);
(2) $\tilde{\gamma}'(n,n_k)$ given in expression (36); and
(3) $\tilde{\phi}(n,n_k)$ given in expression (37).

Although generating these functions is numerically challenging, it only needs to be done over the narrow range of n and n_k associated with the feature. This is illustrated in Fig. 3, which identifies the small ranges of n and n_k over which significant corrections would occur for a model of the first feature.

Our technique is more time consuming, but also more accurate, than the approximation of Adshead, Hu, Dvorkin, and Peiris [31]. When the two approximations were compared using the total correlator (44) of Hung, Fergusson, and Shellard [42], the result (45) was nearly a 50% degradation of the signal, even when the comparison was restricted to a narrow range around the feature. Accurate modeling is crucial when studying features because they produce an oscillating signal, so that even small errors in the phase can significantly degrade the signal. This is especially relevant because the response to a feature is delayed to later crossing wave numbers. Unless the late time phase information is accurately modeled, trying to boost the signal by including the delayed response will actually reduce the measured signal.

In Sec. IV we presented a slight elaboration of a model due to Starobinsky [43] for which the crucial contribution (14) can be computed exactly, without any

approximation [44–46]. In our model $\epsilon(n)$ jumps from ϵ_1 to ϵ_2 and then falls back down after an interval Δn, hence the name "square well model." Expression (60) gives the exact result for the bispectrum of the square well model. However, taking the inessential factors of ϵ to zero produces a simpler and more transparent result (69), which is almost as accurate. A consequence of the sharp transitions is the persistence of oscillations for wave numbers that experience horizon crossing long after the transition. We regarded this as an artifact of the square well approximation, and truncated the late oscillations. For a different point of view we recommend the study of Adshead, Dvorkin, Hu, and Lim [32].

Figure 4 shows that the power spectra of the square well model agree with that of the step model over the narrow range of $170.8 < n < 173$. However, the bispectra they produce are very different. We found a total shape correlator (72) of only about one-third. This underlines the importance of knowing the history $\epsilon(n)$ in addition to accurately modeling the response to it.

ACKNOWLEDGMENTS

This work was partially supported by the European Union's Seventh Framework Programme (FP7-REGPOT-2012-2013-1) under Grant Agreement No. 316165; by the European Union's Horizon 2020 Programme under Grant Agreement No. 669288-SM-GRAV-ERC-2014-ADG; by NSF Grants No. PHY-1506513, No. 1806218, and No. 1912484; and by the UF's Institute for Fundamental Theory.

[1] V. F. Mukhanov and G. V. Chibisov, Pis'ma Zh. Eksp. Teor. Fiz. **33**, 549 (1981) [JETP Lett. **33**, 532 (1981)].
[2] R. P. Woodard, Rep. Prog. Phys. **72**, 126002 (2009).
[3] A. Ashoorioon, P. S. Bhupal Dev, and A. Mazumdar, Mod. Phys. Lett. A **29**, 1450163 (2014).
[4] L. M. Krauss and F. Wilczek, Phys. Rev. D **89**, 047501 (2014).
[5] N. Aghanim *et al.* (Planck Collaboration), arXiv:1807.06209.
[6] P. A. R. Ade *et al.* (BICEP2 and Keck Array Collaborations), Phys. Rev. Lett. **116**, 031302 (2016).
[7] N. C. Tsamis and R. P. Woodard, Ann. Phys. (N.Y.) **267**, 145 (1998).
[8] T. D. Saini, S. Raychaudhury, V. Sahni, and A. A. Starobinsky, Phys. Rev. Lett. **85**, 1162 (2000).
[9] T. Padmanabhan, Phys. Rev. D **66**, 021301 (2002).
[10] S. Nojiri and S. D. Odintsov, Gen. Relativ. Gravit. **38**, 1285 (2006).
[11] R. P. Woodard, Lect. Notes Phys. **720**, 403 (2007).
[12] Z. K. Guo, N. Ohta, and Y. Z. Zhang, Mod. Phys. Lett. A **22**, 883 (2007).
[13] A. Ijjas, P. J. Steinhardt, and A. Loeb, Phys. Lett. B **723**, 261 (2013).
[14] A. H. Guth, D. I. Kaiser, and Y. Nomura, Phys. Lett. B **733**, 112 (2014).
[15] A. Linde, https://dx.doi.org/10.1093/acprof:oso/9780198728856.003.0006.
[16] A. Ijjas, P. J. Steinhardt, and A. Loeb, Phys. Lett. B **736**, 142 (2014).
[17] P. A. R. Ade *et al.* (Planck Collaboration), Astron. Astrophys. **594**, A20 (2016).
[18] J. Torrado, B. Hu, and A. Achucarro, Phys. Rev. D **96**, 083515 (2017).
[19] J. Martin and C. Ringeval, J. Cosmol. Astropart. Phys. 08 (2006) 009.
[20] L. Covi, J. Hamann, A. Melchiorri, A. Slosar, and I. Sorbera, Phys. Rev. D **74**, 083509 (2006).
[21] J. Hamann, L. Covi, A. Melchiorri, and A. Slosar, Phys. Rev. D **76**, 023503 (2007).
[22] D. K. Hazra, A. Shafieloo, G. F. Smoot, and A. A. Starobinsky, J. Cosmol. Astropart. Phys. 08 (2014) 048.
[23] D. K. Hazra, A. Shafieloo, G. F. Smoot, and A. A. Starobinsky, J. Cosmol. Astropart. Phys. 09 (2016) 009.
[24] A. Achcarro, J. O. Gong, G. A. Palma, and S. P. Patil, Phys. Rev. D **87**, 121301 (2013).
[25] D. J. Brooker, N. C. Tsamis, and R. P. Woodard, Phys. Lett. B **773**, 225 (2017).
[26] D. J. Brooker, N. C. Tsamis, and R. P. Woodard, Phys. Rev. D **96**, 103531 (2017).
[27] J. M. Maldacena, J. High Energy Phys. 05 (2003) 013.
[28] J. R. Fergusson and E. P. S. Shellard, Phys. Rev. D **76**, 083523 (2007).
[29] J. R. Fergusson and E. P. S. Shellard, Phys. Rev. D **80**, 043510 (2009).
[30] P. A. R. Ade *et al.* (Planck Collaboration), Astron. Astrophys. **594**, A17 (2016).
[31] P. Adshead, W. Hu, C. Dvorkin, and H. V. Peiris, Phys. Rev. D **84**, 043519 (2011).
[32] P. Adshead, C. Dvorkin, W. Hu, and E. A. Lim, Phys. Rev. D **85**, 023531 (2012).
[33] D. K. Hazra, L. Sriramkumar, and J. Martin, J. Cosmol. Astropart. Phys. 05 (2013) 026.
[34] D. J. Brooker, N. C. Tsamis, and R. P. Woodard, J. Cosmol. Astropart. Phys. 04 (2018) 003.
[35] A. R. Liddle, P. Parsons, and J. D. Barrow, Phys. Rev. D **50**, 7222 (1994).
[36] V. F. Mukhanov, H. A. Feldman, and R. H. Brandenberger, Phys. Rep. **215**, 203 (1992).
[37] A. R. Liddle and D. H. Lyth, Phys. Rep. **231**, 1 (1993).
[38] D. S. Salopek, J. R. Bond, and J. M. Bardeen, Phys. Rev. D **40**, 1753 (1989).

[39] M. G. Romania, N. C. Tsamis, and R. P. Woodard, J. Cosmol. Astropart. Phys. 08 (2012) 029.
[40] J. A. Adams, B. Cresswell, and R. Easther, Phys. Rev. D **64**, 123514 (2001).
[41] M. J. Mortonson, C. Dvorkin, H. V. Peiris, and W. Hu, Phys. Rev. D **79**, 103519 (2009).
[42] J. Hung, J. R. Fergusson, and E. P. S. Shellard, arXiv:1902.01830.
[43] A. A. Starobinsky, Pis'ma Zh. Eksp. Teor. Fiz. **55**, 477 (1992) [JETP Lett. **55**, 489 (1992)].
[44] F. Arroja, A. E. Romano, and M. Sasaki, Phys. Rev. D **84**, 123503 (2011).
[45] J. Martin and L. Sriramkumar, J. Cosmol. Astropart. Phys. 01 (2012) 008.
[46] F. Arroja and M. Sasaki, J. Cosmol. Astropart. Phys. 08 (2012) 012.